A NUMERICAL STUDY ON THE INFLUENCE OF MIXING INTENSITY ON NOx FORMATION

M. Kraft, H. Fey,
Fachbereich Chemie, Universität Kaiserslautern,
Erwin Schrödinger Straße, D 67663 Kaiserslautern, FRG
mkraft@rhrk.uni-kl.de, fey@mathematik.uni-kl.de

A. Schlegel, J.-Y. Chen,
Department of Mechanical Engineering,
University of California at Berkeley, Berkeley, CA 94720, USA
schlegel@pyrolab.me.berkeley.edu, jychen@euler.me.berkeley.edu

H. Bockhorn
Institut für Chemische Technik, Universität Karlsruhe
Kaiserstraße 12, D 76128 Karlsruhe, FRG
bockhorn@ict.uni-karlsruhe.de

Keywords *NOx formation, PDF, Binomial Langevin mixing model, gas turbine combustion*

Abstract

A "Partially Stirred Plug Flow Reactor" model (PaSPFR) has been developed to study the influence of varying intensities of turbulent mixing on NOx formation describing the combustion process during turbulent mixing of two separate flows (i.e. fuel and hot oxidizer) in a tubular flow reactor. This PaSPFR model consists of two submodels for the time evolution of the mass fraction for chemical species and enthalpy which account for turbulent mixing and chemical reactions respectively. Mixing in the combustion chamber is modelled assuming statistically homogeneous and isotropic turbulence via the binomial Langevin mixing model extended to several scalars. Chemistry is modelled using a detailed chemical mechanism of elementary reactions. These two models are incorporated into a Fokker Planck type of equation. In order to calculate its solution a Monte Carlo simulation is performed where equivalent stochastic differential equations for each particle have to be solved. The PaSPFR model is then used to perform a detailed analysis of the sensitivity of reaction paths to various degrees of mixing intensities. The results indicate that the formation pathways of NO formation are sensitive to the mixing intensities. With decreasing mixing intensities, the formation of NO is shifted from the Fenimore reaction channel towards the N_2O channel and the Zeldovich channel. Nevertheless, the total NOx emissions after complete burnout have been found to be influenced only slightly, or even tend to decrease with less intense mixing.

1 Introduction

In many circumstances it is desirable to inject additional fuel, or mixtures of fuel and air into a hot stream of combustion products. For example, in catalytically stabilized combustion for modern gas turbines (i.e. turbine inlet temperatures > 1700K), not all of the fuel can be burnt within the catalyst without deactivating or melting the catalyst. Thus only part of the fuel consumption takes place in the catalyst (e.g. 80 %) and the remaining fuel has to be injected into a hot preburnt mixture [15, 13]. Another example of additional fuel injection is the "sequential combustor system" where, to improve the overall efficiency of gas turbines, a second combustion chamber is employed after the first stages of the turbine (e.g. ABB GT24). In this second combustion chamber it is necessary to inject fuel into a hot stream of combustion products. With todays understanding of combustion, the way of injection (i.e. the mixing with the hot combustion products) has a great influence on the amount of NOx generated in the subsequent combustion zone. In the ideal case, mixing of fuel and hot combustion products should be completed prior to self-ignition. This is to achieve overall lean conditions which lead to overall low combustion temperatures and low NOx emissions. In contrast, insufficient mixing prior to combustion is supposed to result in large temperature differences and therefore in increased NOx emissions. In a

technical application of such a second stage combustor, it is hardly possible to achieve perfect mixing at high pressures and/or high product temperatures before to self-ignition, since ignition delay times are very small under these conditions. As a consequence, turbulent mixing and chemical reactions will occur simultaneously. It is therefore of great interest to determine the interaction of the turbulent mixing and the combustion process as well as its impact on NOx formation. In this work, a "Partially Stirred Plug Flow Reactor" model (PaSPFR) [11] is applied to investigate this interaction. It is a combination of a simple turbulent mixing approach with a detailed chemistry submodel for fuel oxidation and NOx formation. This work supplements the investigation of the influence of unmixedness in a "Partially Stirred Reactor" PaSR [3].

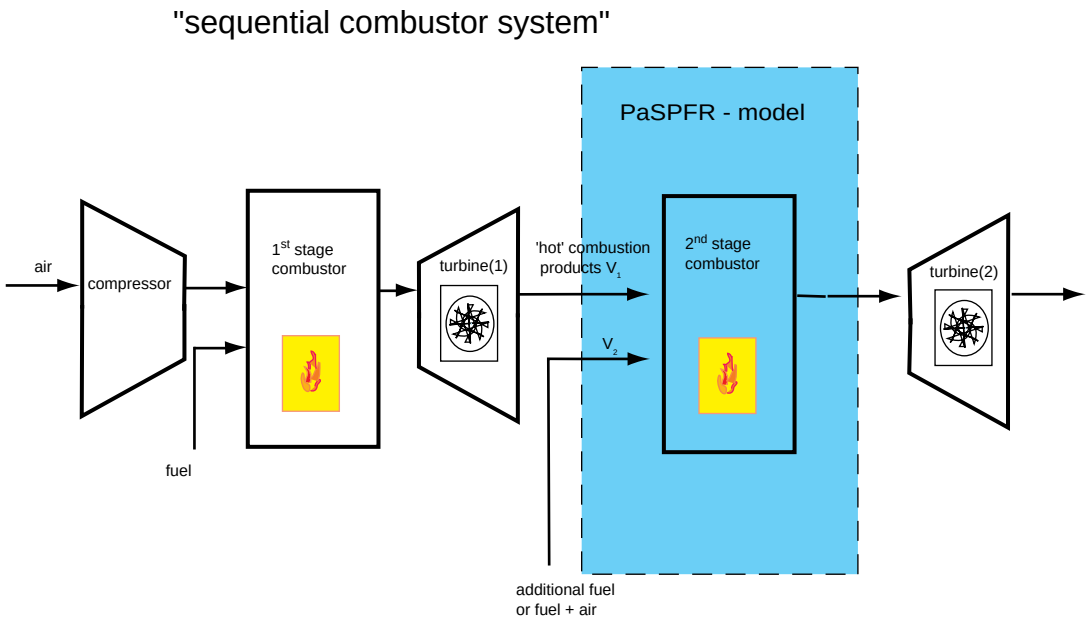

Figure 1: Principle of the "sequential combustor system". To improve overall efficiency, a second combustion chamber is employed after the first stages of a gas turbine. Thereby, additional fuel or a mixture of fuel and air $\dot{V}_2$ have to be injected and mixed into the hot combustion products $\dot{V}_1$ of the previous stages. This second stage combustor is described as a "Partially Stirred Plug Flow Reactor" (PaSPFR), where mixing and chemical reactions occur simultaneously.

2 Modelling

Modelling the interaction of a complex set of chemical reactions and high Reynolds number turbulent fluid flow typical for gas turbine combustion is a challenging task. If the emphasis is on the formation of pollutants such as NOx a full chemistry model is prohibitive. Direct numerical simulation is not feasible due to high computational costs and storage requirements. Even a probability density function (PDF) modelling approach of a "real" gas turbine combustion chamber with boundary effects, swirling inhomogeneous flow by far exceeds computational capacities. Therefore, severe simplifications have to be made to be able to study the interaction of turbulence and detailed chemistry with respect of NOx formation. The second combustion chamber is assumed to be an ideal, turbulent, adiabatic, constant, pressure, tubular flow reactor. It is assumed that there are no boundary effects and the turbulence created at the inlet is homogeneous, isotropic, stationary, and decaying along the reactor axis. The turbulence is characterized by the decay time of the velocity fluctuations $\tau = k/\varepsilon$. k represents the turbulent kinetic energy and ε the dissipation rate. The turbulent time τ is assumed to be fixed and proportional to the decay time of the scalar fluctuations $\tau = C_\phi \tau_\phi$. As suggested in [14] C_ϕ is set $C_\phi = 2.0$. The input into the reactor consisting of two streams with the composition vectors $\underline{\psi}_0^{(1)}$ and $\underline{\psi}_0^{(2)}$ is constant in time.

2.1 Governing Equations

The PaSPFR model is a generalization of the PFR (plug flow reactor), analogous to the PaSR which is a generalization of the PSR (see [2]). It models the time evolution of scalar statistics in a volume element flowing with mean velocity $E(u) = x/t$ along the reactor axis for a given set of initial conditions. Due to the stationary character of the turbulent flow the spatial profiles of scalar statistical quantities along the mean flow axis can be identified with the time evolution of the scalars statistical quantities within the volume element flowing along the reactor axis. This physical system can be described by means of a stochastic process of a random vector $\underline{\phi} = (\phi_1, \ldots, \phi_L)^T = (Y_1, \ldots, Y_K, h^*)^T$ with constant pressure p. Where $Y_k \in [0,1] \quad k = 1, \ldots, K$ are mass fractions of K chemical species and $h^* = \int_{T_0}^{T} c_p \, dT, \quad h^* \in \mathbb{R}$ is the enthalpy contribution due to the heat of the gas mixture in the volume element. The constraint $\sum_{k=1}^{K} Y_k = 1$ defines a manifold $\Re$ of realizable states, called scalar space, for the random vector $\underline{\phi}(t)$. $f_{\underline{\phi}}(\underline{\psi})$ is the joint composition probability density function defined as $P(\underline{\psi} \leq \underline{\phi} \leq \underline{\psi} + d\underline{\psi}) = f_{\underline{\phi}}(\underline{\psi}) d\underline{\psi} = f_{\phi_1 \ldots \phi_L}(\psi_1, \ldots, \psi_L) d\psi_1 \ldots d\psi_L$ where $\underline{\psi}$ is the sampling space vector. For variable density flows the mass density function MDF is defined as $\mathcal{F}(\underline{\psi}; t) = \rho(\underline{\psi}) f_{\underline{\phi}}(\underline{\psi})$. The time evolution of the MDF yields $\mathcal{F}(\underline{\psi}; t) = \int f(\underline{\psi}, t; \underline{\psi}_0, t_0) \mathcal{F}(\underline{\psi}_0; t_0) d\underline{\psi}_0$ where $\mathcal{F}(\underline{\psi}_0; t_0)$ describes the initial distribution at starting time $t = t_0$. $f(\underline{\psi}, t; \underline{\psi}_0, t_0)$ is the transition PDF defined as $f(\underline{\psi}, t; \underline{\psi}_0, t_0) d\underline{\psi} = P(\underline{\psi} \leq \underline{\phi} \leq \underline{\psi} + d\underline{\psi} \mid \underline{\phi}(t_0) = \underline{\psi}_0)$. The equation for the time evolution of the transition probability density is given in ref. [14].

$$\underbrace{\frac{\partial}{\partial t} f}_{\text{change in time}} = -\sum_{l=1}^{L} \left[\underbrace{\frac{\partial}{\partial \psi_l} \left[E\left(\frac{D_l}{\rho} \nabla^2 \phi_l \mid s_t, s_0 \right) f \right]}_{\text{molecular diffusion}} + \underbrace{\frac{\partial}{\partial \psi_l} \left(S_l f \right)}_{\text{chemical source}} \right] \tag{1}$$

The solution of (1) is determined by the initial conditions $f = f(\underline{\psi}, t_0; \underline{\psi}_0, t_0) = \delta(\underline{\psi} - \underline{\psi}_0)$. The first term on the right hand side describes the transport of the transition probability density due to molecular diffusion and the second term describes the transport due to chemical reaction. The expectation of the scalar flux $E\left(\frac{D_l}{\rho} \nabla^2 \phi_l \mid s_t, s_0 \right)$ is conditional on $s_0 = \{\underline{\phi}(t_0) = \underline{\psi}_0\}$ and $s_t = \{\underline{\phi}(t) = \underline{\psi}\}$. D_l $(l = 1, \ldots, L-1)$ is the mass diffusivity of the l-th species χ_l, ρ is the gas density, and $D_L = \frac{\lambda}{c_p}$ represents the thermal diffusivity. The conditional expectation of the molecular diffusion is not known and needs to be replaced by a suitable model. The second term in the above equation desribes the influence of chemical reactions on the transition PDF. $S_l = \rho^{-1} \dot{\omega}_l(\underline{\psi}) W_l \, (l = 1, \ldots, L-1)$ where $\dot{\omega}_l(\underline{\psi})$ is the molar production rate and W_l is the molar weight of the l-th species χ_l. Source term for the enthalpy is $S_L = \rho^{-1} \sum_{k=1}^{K} h_{0k} W_k \dot{\omega}_k(\underline{\psi})$ where h_{0k} is the formation enthalpy of the k -th species.

2.1.1 Molecular diffusion term

The molecular diffusion term in the PDF equation describes the combined action of turbulent straining and molecular transport. A model for the molecular diffusion term must satisfy a number of conditions. It should not alter the scalar mean value and produce the correct decay velocity of variance for a chemically inert flow. The time evolution of the random vector $\underline{\phi}$ has to stay within the manifold $\Re$ and the fluxes on $\partial\Re$ have to point inward $\Re$ to account for the bounded scalar field. Dimensional consistence as well as coordinate system independence must be fulfilled. Additionally linearity and independence of inert dynamically passive scalars also have to be satisfied. Results of direct numerical simulation of stationary homogeneous isotropic turbulence of a single inert scalar in [4] gives evidence that the PDF relaxes asymptotically to a Gaussian distribution. Among all the existing models for molecular diffusion only the amplitude mapping closure model [1] and the binomial Langevin (BL) [16, 8] lead to the correct Gaussian asymptotics. In the subsequent part the binomial Langevin model is used for simulation studies. There, the decay of the fluctuations is modelled by a deterministic drift which contracts the PDF to its mean and a noise which blurs the PDF to have a Gaussian asymptotic behaviour. The operator $\partial_b^2 / \partial_b \psi_l^2$ is a symbolic notation for a generator of a binomial stochastic process which tends to a diffusion process

for decaying fluctuations. This guarantees that the boundedness condition for the scalars is satisfied.

$$-\sum_{l=1}^{L}\frac{\partial}{\partial\psi_l}\left(E(\frac{D_l}{\rho}\nabla^2\phi_l|s_t,s_0)f\right)=-\sum_{l=1}^{L}\frac{\partial}{\partial\psi_l}(A_l(\underline{\psi})f)+\sum_{l,m=1}^{L}\frac{1}{2}\frac{\partial_b^2}{\partial_b\psi_l\partial_b\psi_m}(B_{lm}(\underline{\psi})f) \tag{2}$$

with

$$A_l(\underline{\psi}) = -\frac{1}{2}\left[1+k\left(1-\frac{D(\phi_l)}{\psi_{l*}^2}\right)\right]\frac{C_\phi}{\tau}\left(\psi_l-E(\phi_l)\right) \tag{3}$$

$$B_{lm}(\underline{\psi}) = \begin{cases} k\left[1-\frac{(\psi_l-E(\phi_l))^2}{\psi_{l*}^2}\right]\frac{C_\phi}{\tau}D(\phi_l) & : \quad l=m \\ 0 & : \quad l\neq m \end{cases} \tag{4}$$

$$\psi_{l*}=\begin{cases} (\psi_l^{\max}-E(\phi_l)) & : \quad (\psi_l-E(\phi_l))\geq 0 \\ (\psi_l^{\min}-E(\phi_l)) & : \quad (\psi_l-E(\phi_l))<0 \end{cases} \tag{5}$$

and the empirical constant $k=0.1$ and $C_\phi=2.0$ as suggested in e.g. [14]. In the above equations $E(\phi)$ and $D(\phi)$ denote the mean and the variance of the random variable ϕ. The coefficients $A(\psi_l)$ and $B(\psi_l)$ are chosen in such a way to fit the solution of (2) to the results of the DNS in [4]. The idea behind this choice is to have for small times a scalar dependent coefficient of diffusion which should be zero for extreme values of scalar fluctuations and maximum for values of ψ_l in the neighborhood of $E(\phi_l)$. The drift coefficient is also modified to get the right decay of variance.

2.1.2 Chemical source term

The molar production rate $\dot{\omega}_l$ is a function of the composition vector $\underline{\phi}=(Y_1,..,Y_K,h^*)$ and is described by I elementary reversible reactions involving K chemical species.

$$\sum_{k=1}^{K}\nu'_{ki}\chi_k \rightleftharpoons \sum_{k=1}^{K}\nu''_{ki}\chi_k \tag{6}$$

The stoichiometric coefficients ν_{ki} are integers and χ_k is the symbol for the k -th species. The reaction rate of reaction i is given as $q_i=q_i(\underline{Y},T)$. The temperature T is a function of enthalpy and composition variables $T=T(\underline{Y},h^*)$. The integrated reaction rates over the time interval $[0,t]\,s$ is given as $Q_i=\int_0^t q_i dt$. These two variables are statistically described by their probability densities $f_{\underline{q}}(q_1,q_2,q_3,\ldots,q_I;t)\,, f_{\underline{Q}}(Q_1,Q_2,Q_3,\ldots,Q_I;t)$. These densities are approximated when evaluating the chemical source terms of the representative stochastic particles using the CHEMKIN library [10, 9]. From these densities the mean conversion $E(Q_i)(t)=\int Q_i f_{Q_i}(Q_i,t)\,dQ_i$ of the reaction i can be calculated. In addition to the rate of progress variable q_i the molar production rate of a species k in reaction i, $\dot{w}_{ki}=(\nu''_{ki}-\nu'_{ki})\,q_i$, the conversion of species k in reaction i in the time interval $[0,t]s$, $w_{ki}=\int_0^t \dot{w}_{ki}\,dt$, and the overall production of the species k given as $w_k=\sum_{i=1}^{I} w_{ki}$ can be calculated to describe the dynamic of the chemical reactions. The estimators of the expectations and the higher statistical moments can be obtained from the discrete representation of $f_{\underline{q}}$ and $f_{\underline{Q}}$. Carbon-hydrogen-oxygen chemistry of natural gas ignition and flames is modelled using the GRI-Mech 2.1 chemical mechanism [6]. Version 2.1 expands GRI-Mech 1.2 [5] by including nitrogen chemistry. It consists of complex set of 279 elementary chemical reactions and 49 chemical species. GRI-Mech 2.1 was developed optimizing the nitrogen chemistry relevant to natural gas flames and reburning. It is an improvement for the experiments modelled over previous attempts to describe NOx formation and removal in natural gas flames, for example the 1989 Miller and Bowman mechanism [12]. Still GRI-Mech 2.1 is only a preliminary starting point that can not be applied with anything like the degree of confidence that can be attached to the version 1.2 carbon-hydrogen-oxygen chemistry.

2.1.3 Numerical treatment

The transport equation for the transition probability density (1) - (5) is a Fokker Planck equation and can be written in the following way.

$$\frac{\partial}{\partial t} f(\underline{\psi}, t; \underline{\psi_0}, t_0) = (P_A + P_B + P_S) f(\underline{\psi}, t; \underline{\psi_0}, t_0) \tag{7}$$

and the initial conditions $f_0 = f(\underline{\psi}, t_0; \underline{\psi_0}, t_0) = \delta(\underline{\psi} - \underline{\psi_0}) = \prod_{l=1}^{L} \delta(\psi_l - \psi_{l0})$. The operators $P_.$ represent the transport of the transition probability density due to chemical reaction and molecular diffusion. P_A describes the deterministic drift towards the mean value, P_B describes the stochastic fluctuations, and P_S represents the influence of the chemical reaction on the transition probability density function. For example from (2) follows that

$$P_A = \sum_{l=1}^{L} \left(\frac{\partial}{\partial \psi_l} A_l(\underline{\psi}) I + A_l(\underline{\psi}) \frac{\partial}{\partial \psi_l} \right). \tag{8}$$

where I is the identity operator. In order to solve equation (7) the solution procedure is divided in several steps. Therefore we approximate the solution operator S_{t,t_0} with $\frac{\partial}{\partial t} f(., t; ., .) = S_{t,t_0} f_0$ of (7) in the following way $S_{t,t_0} \approx S^{P_A}_{t,t_0} S^{P_B}_{t,t_0} S^{P_S}_{t,t_0}$. This results in

$$f^*(t) = S^{P_A}_{t,t_0} f_0 \tag{9}$$

$$f^{**}(t) = S^{P_B}_{t,t_0} f^*(t) \tag{10}$$

$$f^{***}(t) = S^{P_S}_{t,t_0} f^{**}(t) \tag{11}$$

This operator splitting technique leads to three transport equations for the transition PDF. These have to be solved successively. Due to the high dimension $L = 50$ of the transition PDF we choose a Monte Carlo technique. Therefore we approximate the initial distribution by N particles.

$$F(\underline{\psi}, t_0) \approx F_N(\underline{\psi}, t_0) = \sum_{n=1}^{N} \Delta m^n \prod_{l=1}^{L} \delta(\psi) - \psi^n_{l0}) \tag{12}$$

Here Δm^n is the individual particle weight according to its mass. Each particle is now an initial condition for the stochastic process corresponding to equations (9)-(11). Each equation corresponds to a fractional step in the solution procedure. For the first fractional step we have to solve for each particle the initial value problem.

$$\frac{d\psi^n_l}{dt} = A_l(\underline{\psi}^n(\underline{\psi}^n_0, t)) \qquad \psi^n_l(\psi^n_{l0}, t_0) = \psi^n_{l0} \qquad n = 1, \ldots, N \tag{13}$$

The second step corresponds to simulating the stochastic noise by solving a system of stochastic differential equations with the result of (13) as initial value. The outcome of the second fractional step serves as initial condition for the last and third fractional step which describes the influence of the chemical reactions. For this a system of stiff ordinary differential equations has to be solved. The N particles $\underline{\psi}^n(\underline{\psi}^n_0, t) \quad n = 1, \ldots, N$ approximate the mass density function MDF at time t.

$$F(\underline{\psi}, t) \approx F_N(\underline{\psi}, t) = \sum_{n=1}^{N} \Delta m^n \delta(\underline{\psi} - \underline{\psi}^n(\underline{\psi}^n_0, t)). \tag{14}$$

This solution procedure introduces at several points numerical errors. The first source is approximating the initial MDF by particles. In this work this error vanishes because of the choice of the initial conditions which is a composition of two delta functions. The second source of error enters the numerical solution through the operator splitting technique. This simple technique is described in [14] and it introduces a first order error. In each fractional step the solution operator $S^{P_.}_{t,t_0}$ has to be approximated by a time discrete numerical method.

$$S^{P_.}_{t,t_0} = \mathcal{H}^{P_.}_{\Delta t,t_0} \tag{15}$$

This approximation also introduces an numerical error. In case of $S_{t,t_0}^{P_A}$ an analytic solution can be found because it describes a linear drift. This solution is a function of moments of ϕ_l like mean $E(\phi_l)$ and variance $D(\phi_l)$. These moments have to be estimated from the discrete particle ensemble which also introduces an numerical error. This error is proportional to the standard deviation $\sqrt{D(\phi_l)}$ and decreases with the square root of the number of particles N. To obtain a numerical approximation of the noise operator $S_{t,t_0}^{P_B}$ a numerical scheme for the corresponding system of stochastic differential equations is applied [16]. We choose an equidistant time step $\Delta t = t_{j+1} - t_j \quad j = 0, \ldots, J-1$ and a stochastic increment $\Delta W_{blj} = W_{blj}\Delta t$. W_{blj} is a binomial distributed random variable therefore the statistical moments of the stochastic increment are $E(\Delta W_{bj}) = 0$ and $E((\Delta W_{bj})^2) = \Delta t$. Starting from an initial vector $\underline{\psi}^n(\underline{\psi_0^n}, t_0) = \underline{\psi_0^n}$ we obtain an approximation for $\underline{\psi}^n(\underline{\psi_0^n}, t_{j+1})$ applying the following scheme.

$$\hat{\psi}_l^n(t_{j+1}) = \hat{\psi}_l^n(t_j) + \sqrt{\hat{B}_{ll}(\hat{\psi}_l^n(t_j)}\Delta W_{blj} \tag{16}$$

$\hat{\psi}_l^n(t_{j+1})$ is called the Euler(- Maruyama) approximation of $\underline{\psi}^n(\underline{\psi}_0^n, t_{j+1})$. Approximating B_{ll} by $\hat{B}_{ll}$ introduces a numerical error because mean and variances have to be estimated. In addition, a random or statistical error is introduced when calculating the stochastic increment ΔW_{blj}. A further problem is the violation of physical principles. Using a binomial distribution preserves boundedness of the scalars, i.e. $\psi_l \in [0, 1]$. In the limit for $D(\underline{\phi}) \to 0$ the random number W_{bj} is normal distributed and therefore imposes the right asymptotic behaviour on the PDF. Although the components of the scalar property vector are bounded they do not need to be inside the manifold $\Re$ which was defined by the sum of all chemical species mass fractions is equal to one for each particle. Moreover, due to the finite number of particles (in this simulation we have $N = 150$) the estimated mean $\hat{E}(\underline{\phi})$ is not constant after proceeding form one time step to the next. This is clearly unphysical. Hence a correction procedure is employed to fulfill $\sum_{l=1}^{L-1} \psi_l^n = 1$ and $\hat{E}(\underline{\phi}(t_j)) = \hat{E}(\underline{\phi}(t_{j-1}))$. In this procedure the particle properties are scaled by a correction factor to meet the first condition. The second condition is also achieved by a scaling. This two scaling procedures are then iterated until the error is small enough. Finally the last fractional step which corresponds to the operator $S_{t,t_0}^{P_S}$ has to be approximated. This operator describes the chemical source term. For each particle a system of stiff ordinary differential equations has to be solved. This is done using DASSL stiff ODE integrator as part of the SENKIN program provided by Sandia National Laboratories [9]. DASSL employs a variable stepsize, variable order fixed leading coefficient implementation of backward differential formulas.

2.2 Initial Conditions

In the present study, only one set of inlet gas compositions and temperatures is used for the two streams V_1 and V_2 (table 1). V_2 represents the "hot combustion products" from an earlier combustion chamber, referred to as "exhaust" and V_1 is the injected stream of fuel and nitrogen, referred to as "fuel". The volume flow ratio $\dot{V}_1/\dot{V}_2$ [nm3/s] is fixed at 0.17. The pressure is fixed at $1\,atm.$. This set of inlet conditions yields adiabatic combustion temperatures of 1500°C after complete combustion. This is to meet turbine inlet temperatures of modern gas turbines. The only parameter varied in this study is the characteristic turbulent mixing time τ. It corresponds to the degree of mixing intensity in the tubular flow reactor. Numerical simulations are performed for $\tau = 0s, 0.008s, 0.025s$ and $0.05s$ for which the characteristic physical and chemical times are of the same order of magnitude. The limiting case of $\tau = 0s$ implies infinitely fast mixing, i.e. a "perfectly premixed" mixture of V_1 and V_2 enter the combustion chamber. In this case, the PaSPFR model describes a plug flow reactor (PFR) where no mixing occurs in the combustion process. The perfectly premixed inlet composition and temperature are shown in table 1 as "PFR" inlet conditions. As initial condition for the MDF transport equation we have the joint composition mass density function at time $t = t_0$.

$$\mathcal{F}(\underline{\psi}; t_0) = \mathcal{F}_0(\underline{\psi}) = \frac{1}{2}\rho(\underline{\psi})\left(\delta(\underline{\psi} - \underline{\psi}_0^{(1)}) + \delta(\underline{\psi} - \underline{\psi}_0^{(2)})\right) \tag{17}$$

In equation (17) the vectors $\underline{\psi}_0^{(1)}$ and $\underline{\psi}_0^{(2)}$ are the mass fraction and enthalpy composition vectors of stream V_1 and stream V_2 respectively.

	Fuel	Exhaust	PFR
	$\dot{V}_1$	$\dot{V}_2$	
X(N_2)	0.750	0.753	0.752
X(O_2)	0.000	0.167	0.151
X(H_2O)	0.000	0.052	0.047
X(CO_2)	0.000	0.028	0.025
X(CH_4)	0.250	0.000	0.023
Temp.	770 K	1303 K	1244 K

Table 1: Inlet conditions to the PaSPFR ($\dot{V}_1$,$\dot{V}_2$) and the PFR as used in this study. $X(k)$ are mole fractions of the chemical species and the ratio of the volume streams between V_1 and V_2 is set to be $\dot{V}_1/\dot{V}_2 = 0.17$.

3 Results and Discussion

In the following sections, we first discuss in detail the ignition process and the different channels of NO formation for the limiting case $\tau = 0s$, i.e. a "Plug Flow Reactor" (PFR), where both flows are mixed instantaneously at the inlet of the combustion chamber (at t=0). In a second step, computational results obtained with the PaSPFR model are shown to demonstrate the influence of different mixing intensities on the combustion process and the NO formation. The characteristic turbulence times are chosen such that mixing and combustion occur simultaneously.

3.1 The PFR case

The time evolution of mass fractions of some important chemical species is displayed in figures 3,4,5,6, and 7 for the time interval $[0, 5]$s. The PFR case can be found in the diagrams of the estimated mean mass fraction for $\tau = 0$s. After 0.018s the homogeneous gas mixture ignites as indicated by a sharp peak in the OH mass fraction time evolution. During ignition carbon monoxide is formed and then oxidized to CO_2. After ignition CH_4 is completely consumed in the given fuel lean environment. Nitrogen oxides are formed during the combustion process. Figure 2 shows the most important reaction channels under the conditions chosen for this study. The numbers of the reactions correspond to those in the GRI mechanism 2.1. Since the adiabatic combustion temperature is low (1500°C), there is only negligible "post-flame" NO formation, i.e. all of the NO is formed as "prompt-NO" within the combustion zone. The different reactions can be allocated as follows to the three main NO formation mechanisms :

- Zeldovich mechanism

$$\mathrm{N + NO} \rightleftharpoons \mathrm{N_2 + O} \tag{178}$$

$$\mathrm{N + O_2} \rightleftharpoons \mathrm{NO + O} \tag{179}$$

$$\mathrm{N + OH} \rightleftharpoons \mathrm{NO + H} \tag{180}$$

  The Zeldovich mechanism comprises three elementary reactions. The cleavage of the N2 bond by the attack of O-atoms in reaction 178 is the rate determining step. Since reaction 178 has a very high activation energy, NO formation via the Zeldovich mechanism is very temperature dependent. Although combustion temperatures are low under the given conditions, the Zeldovich mechanism plays an important role in NO formation (Fig. 9), since reaction 178 is enhanced by superequilibrium concentrations of O-atoms during the combustion process.

- N_2O mechanism

$$N_2O + O \rightleftharpoons 2NO \quad (182)$$

$$NH + NO \rightleftharpoons N_2O + H \quad (199)$$

In the N_2O mechanism NO is formed via the intermediate species N_2O. For the given initial conditions only reactions 182 and 199 contribute significantly to the NO formation.

- Fenimore mechanism

$$NH + O \rightleftharpoons NO + H \quad (190)$$

$$NH + O_2 \rightleftharpoons NO + OH \quad (195)$$

$$N_2H + O \rightleftharpoons NH + NO \quad (208)$$

$$H + NO + M \rightleftharpoons HNO + M \quad (212)$$

$$HNO + O \rightleftharpoons NO + OH \quad (213)$$

$$HNO + H \rightleftharpoons H_2 + NO \quad (214)$$

$$HNO + OH \rightleftharpoons NO + H_2O \quad (215)$$

$$HNO + O_2 \rightleftharpoons HO_2 + NO \quad (216)$$

The Fenimore mechanism includes a whole set of elementary reactions. Usually, NO formation is initiated by the attack of hydrocarbon radicals CH_i on N_2. Reaction channels of NO formation strongly depend on fuel concentration during the combustion process. Some of the kinetical data for these reactions are still not known exactly. The Fenimore mechanism is not as much temperature dependent as in the Zeldovich mechanism due to lower activation energies. Listed below are only those reactions which contribute significantly to the formation of NO under the given initial conditions.

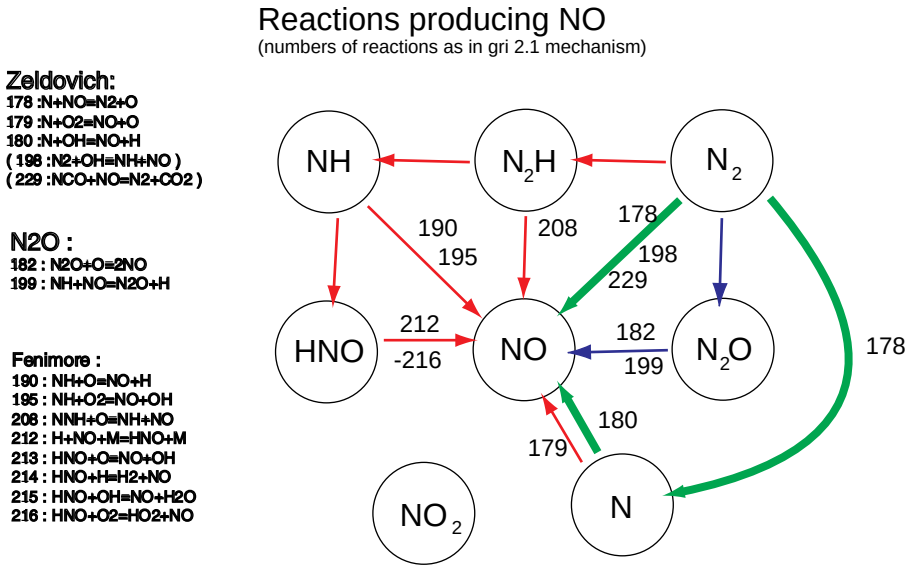

Figure 2: Reaction paths of the perfectly mixed composition

All other reactions involving N-containing species listed in the GRI mechanism are not significant under the prevailing conditions. As a matter of fact, reaction

$$CH + N_2 \quad \rightleftharpoons \quad HCN + N \tag{240}$$

usually regarded as "initial reaction" of the Fenimore mechanism, contributes only negligibly to the formation of N- or HCN-radicals. Nevertheless, the allocation of the reactions to the three NO mechanisms, as found in literature, shall be retained in this study. Figure 9 shows the specific molar production of NO in the PFR ($\tau = 0$) for each of the reactions mentioned above. Approximately 50% of the total NO is produced by the Fenimore mechanism while N_2O and Zeldovich mechanisms contribute 18% and 32% respectively. The integration time is equal to the simulation time of 5s.

3.2 PaSPFR results

In the following the influence of the turbulent mixing on the chemical kinetics is subject of investigations. We shall demonstrate that turbulence acts as a perturbation to the chemical reactions. This perturbation is caused by the stochastic process which alters the evolution of the trajectories of the composition vectors in phase space due to chemical reactions. In order to demonstrate the influence of turbulent mixing on the chemical reactions we vary the turbulent times τ. From the limiting case of the PFR $\tau = 0s$ we move to realistic turbulent time scales $\tau = 0.008s$ which corresponds to very fast mixing and then to $\tau = 0.025s$ an intermediate mixing time and $\tau = 0.05s$ which is slow mixing. The turbulence times are about the same order as the characteristic time for chemical reactions to guarantee that both processes influence each other. This will be demonstrated with the time evolution of the statistical moments estimated from the approximation of the PDF for the important chemical species as well as two dimensional marginal PDF. Additionally the estimations of the overall production of NO from the chemical source term of each particle will give insight on how reaction paths will vary.

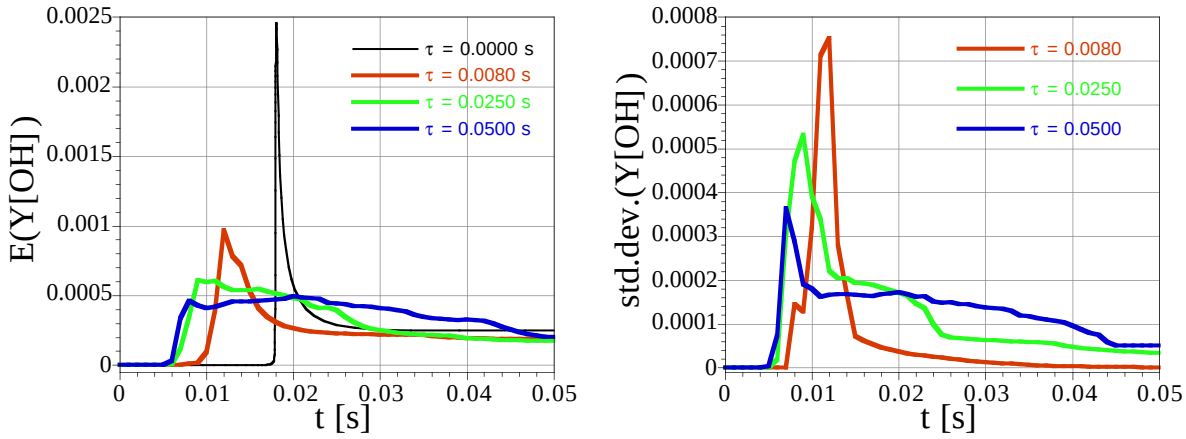

Figure 3: Time evolution of estimated mean and standard dev. of OH mass fraction in the PFR and PaSPFR for different turbulent times.

Fig. 3 shows the time evolution of the estimated mean and standard deviation of OH mass fraction. With decreasing mixing intensity (increasing mixing time τ), ignition delay times decrease significantly. The ignition delay time is defined as the time elapsed between $t = 0s$ and the sudden increase in OH mass fraction. The combustion process, which is very short in the PFR case, is stretched for less intense mixing and the OH peak concentrations are much lower.

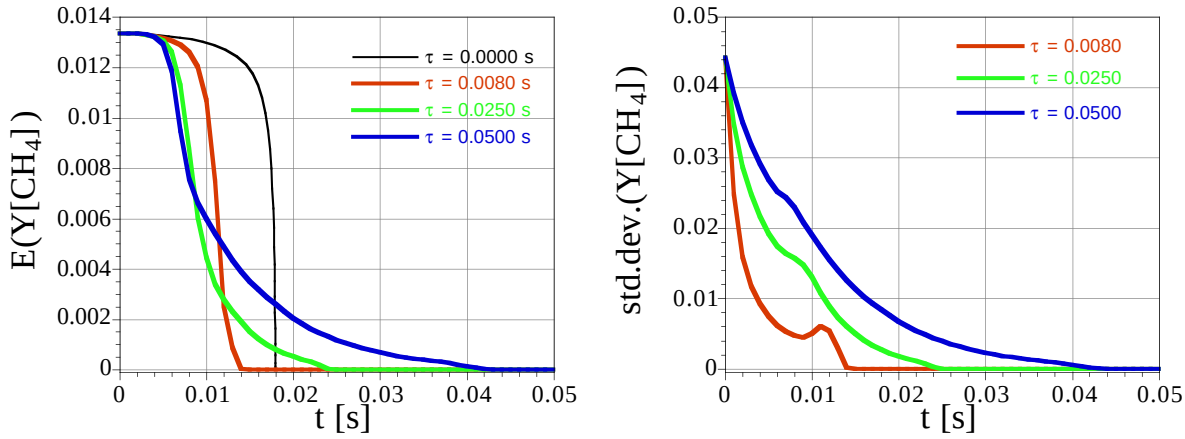

Figure 4: Time evolution of estimated mean and standard dev. of methane in the PFR and PaSPFR for different turbulent times.

Figs. 3, 4 and 5 show, that in all cases the combustion process is fully completed within the calculation time of 50 ms, i.e. all radicals reached their equilibrium concentrations and mass fraction of CO_2 its maximum value. The standard deviation of the species concentration, which is shown in Figs. 3 to 6 as well, is a measure of homogeneity of the mixture. It is important to note, that after completion of the combustion process, all species except NO are fully mixed as well (st. dev. $= 0$). However, the mean NO mass fractions after complete combustion depend only slightly on mixing intensity. This is in contrast to the common expectation that imperfect mixing in the combustion process leads to overall higher NOx emissions.

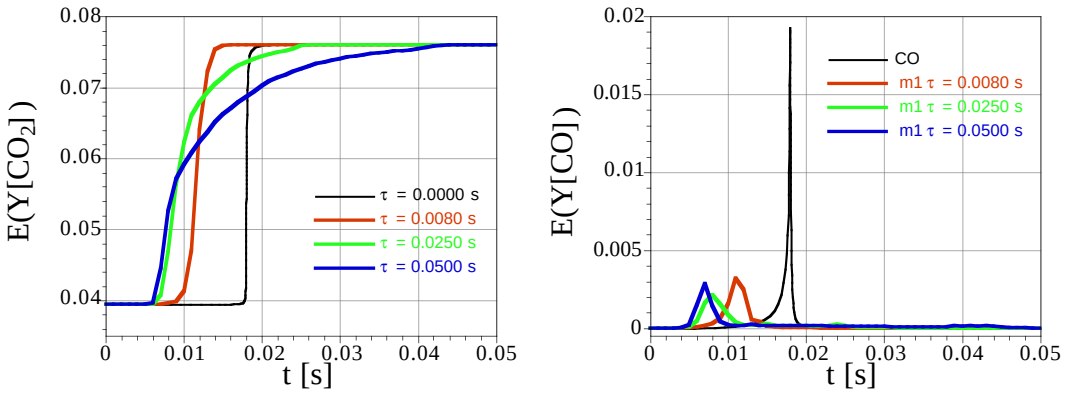

Figure 5: Time evolution of estimated means of carbon dioxide and carbon monoxide in PFR and PaSPFR for different turbulent times.

Figure 8 shows the time evolution of the marginal PDF of temperature and mass fraction NO, $f(T, NO)$, for different mixing times $\tau = 0.008$s and $\tau = 0.05$s. At starting time ($t = 0s$) the two initial states for stream V_1 and V_2 are represented by two groups of particles in the $T - Y(NO)$ plain. These represent the initial double delta PDF. At time $t = 0s$ no NO is present in neither of the two streams. The black

line is the projection of the unperturbated trajectory on the $T - Y(NO)$ plain. At time $t = 0.010s$ in both cases particle have already moved. The binomial Langevin model has two effects on the particles. The deterministic drift moves all particles towards their mean and the noise blurs the delta functions.

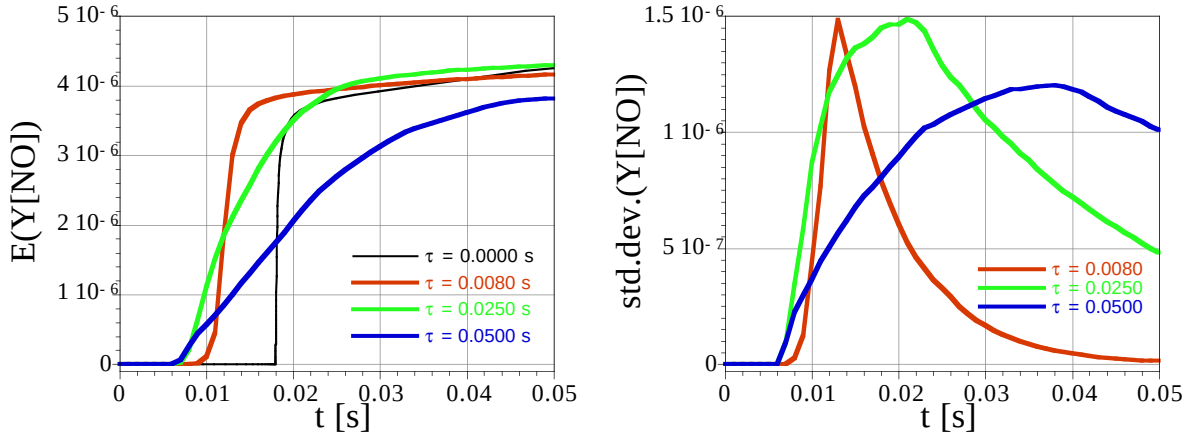

Figure 6: Time evolution of estimated mean and standard dev. of NO in the PFR and PaSPFR for different turbulent times.

In case of $\tau = 0.008$ the contraction has progressed further than in case of slow mixing $\tau = 0.05$. In the fast mixing case particles stay close to the PFR trajectory. The temperature rise of some particles is due to their ignition. At time $t = 0.013s$ one can still distinguish between two composition streams. A little later at $t = 0.015s$ all particles are ignited. At the end of the simulation at time $t = 0.05s$ all particles are close to equilibrium and homogeneously mixed.

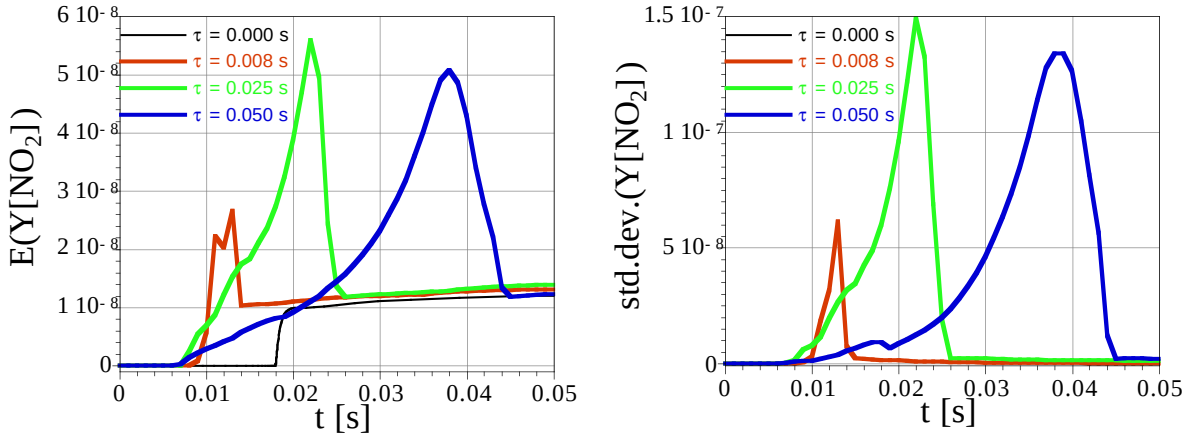

Figure 7: Time evolution of estimated mean and standard dev. of NO_2 in the PFR and PaSPFR for different turbulent times.

In case of slow mixing $\tau = 0.05$ the two streams keep separated much longer and as consequence of this particles are not as close to the PFR trajectory as in the fast mixing case $\tau = 0.008$. Because of slower

mixing fuel and oxygen can not react as fast as in the case of $\tau = 0.008$ and this mixing controlled situation is the reason for the much slower movement of the particles in composition space.

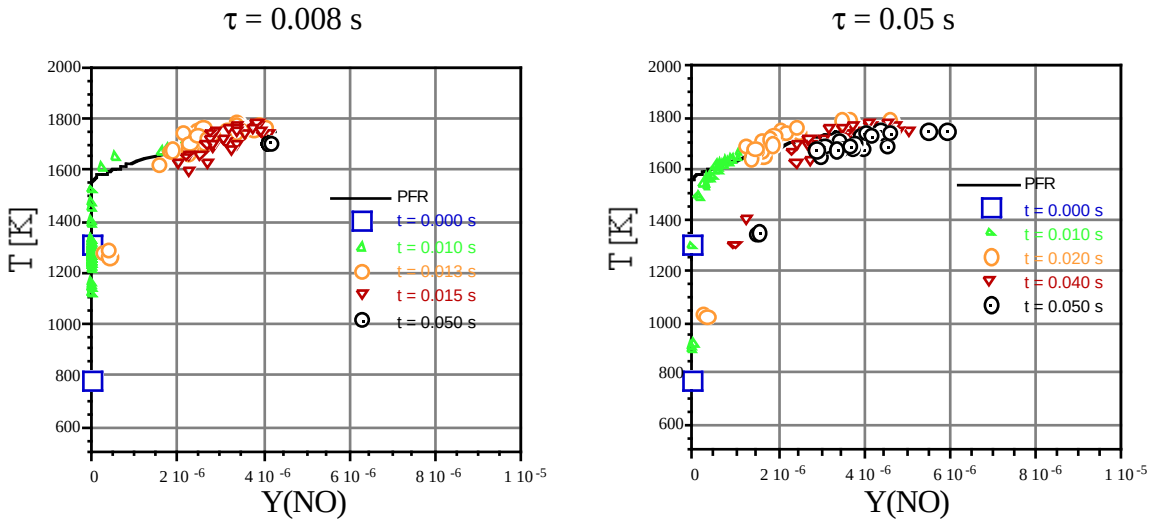

Figure 8: Time evolution at discrete points of time of the marginal two dimensional PDF of NO mass fraction and temperature for different mixing times.

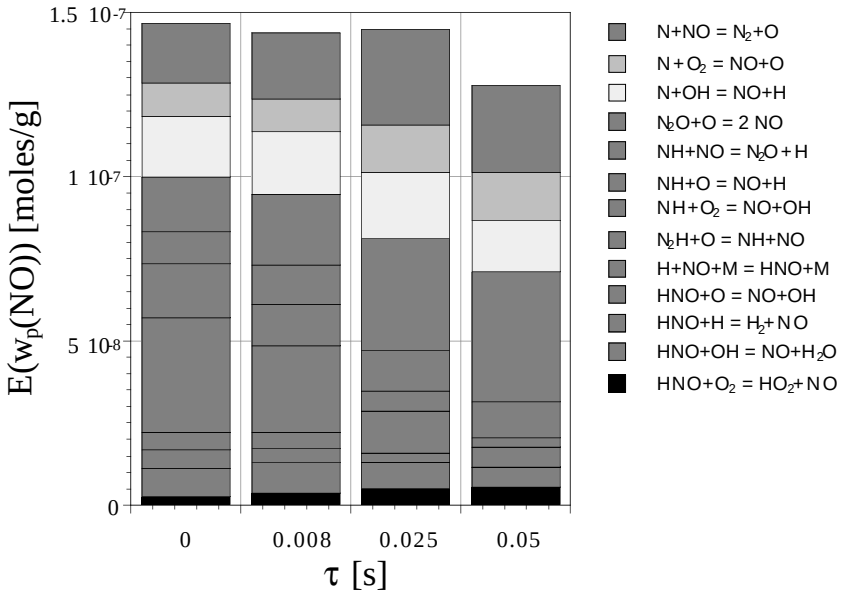

Figure 9: Estimated mean of the overall production of NO for various turbulent mixing times. Simulation time for both the PaSPFR and PFR model is 0.05s.

At time $t = 0.05s$ the mixture is still not homogeneous. Most particles have a lower NO mass fraction than the corresponding value for the faster mixing case. This is in agreement with the time profiles of the estimated means. The strong influence of turbulent mixing on the PDF also effects the overall integrated specific mean molar productions of NO. Estimates of this quantity for various τ are presented in figure 9. The main effect of turbulent mixing is that the NO formation channels vary significantly for the various grades of mixing. In the perfectly mixed case the percentage of Zeldovich, N_2O, and Fenimore formation pathways of the overall production is 32%,18%, and 50% respectively. These percentages change strongly

for increasing turbulent time τ. The percentage of NO formation via the Zeldovich mechanism increases from 32% which corresponds to $4.6 \times 10^{-7}\, moles\, g^{-1}$ for $\tau = 0s$, to 32% for $\tau = 0.008s$, to 43% for $\tau = 0.025s$, and eventually to 45% ($5.8 \times 10^{-7}\, moles\, g^{-1}$) for $\tau = 0.05s$. This increase is due to the molar production growth of reaction 178. This effect is also exhibited in figure 10. There, the mean specific molar fluxes of species which form NO integrated over the simulation time is displayed. On the left side species are listed which contribute to NO formation which leads to a negative molar flux and species which are formed by consuming NO which results in a positive molar flux. The increase of NO production in reaction 178 is reflected by an increase on N_2 consumption for NO formation. For the N_2O mechanism and the Fenimore mechanism the influence of turbulent mixing is even more significant. NO formation via N_2O increases from 18% ($2.7 \times 10^{-7}\, moles\, g^{-1}$) for $\tau = 0$, to 23% for $\tau = 0.008$, to 33% for $\tau = 0.025$, and to 39% ($5.0 \times 10^{-7}\, moles\, g^{-1}$) for $\tau = 0.05$. This strong increase of NO production via the N_2O is almost exclusively caused by reaction 182. In figure 10 also the N_2O mean specific molar flux to NO increases for larger τ. NO production through reaction 199 almost remains constant. The formation of NO via Fenimore mechanism decreases significantly when changing the turbulent time τ. From 50% ($7.3 \times 10^{-7}\, moles\, g^{-1}$) for $\tau = 0$, to 42% for $\tau = 0.008$, to 24% for $\tau = 0.025$, and to 16% ($2.01 \times 10^{-7}\, moles\, g^{-1}$) for $\tau = 0.05$. This very strong decrease of Fenimore NO is mainly due to a decrease of NO productions in reaction 190 and 208. The mean NO contribution of these reactions reduces from $5.1 \times 10^{-7}\, moles\, g^{-1}$ to $0.8 \times 10^{-7}\, moles\, g^{-1}$.

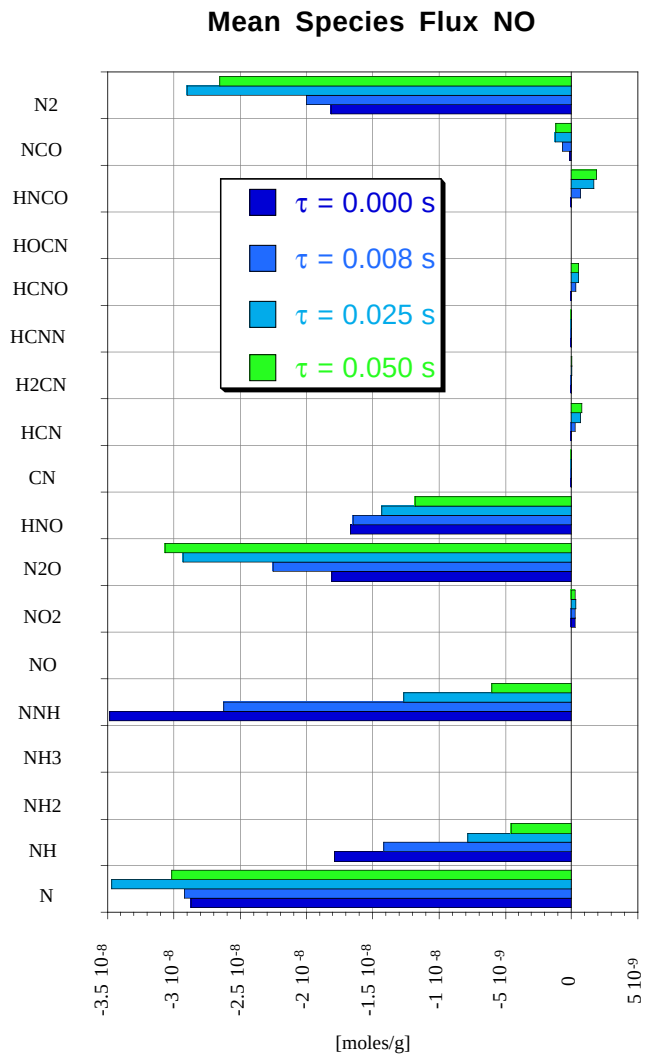

Figure 10: Estimated mean of the integrated species flux to NO for various turbulent mixing times. Integration time interval corresponds to the simulation time, i.e. $0.05s$.

This decrease leads to a significant mean flux reduction of the species NH and N_2H. Another important observation is that NO production in reactions which involve O radicals such as 178 in the Zeldovich mechanism, reaction 182 in the N_2O mechanism and reactions 190 and 208 are all effected significantly by turbulent mixing. This important role of the O radical should be examined closer in future work. The fact that ignition phase changes its character from a short ignition to a long ignition process with less step gradients in the temperature profiles might be responsible for the above observation.

3.3 Conclusions

A "Partially Stirred Plug Flow Reactor" (PaSPFR) model has been developed as a tool to study the influence of turbulent mixing intensity on the combustion process and NO formation. It combines complex C/H/N/O chemistry and the binomial Langevin mixing model assuming homogeneous isotropic turbulence. The model describes simultaneous combustion and mixing of two separate flows in a tubular flow reactor. It is used in this work to simulate the case where additional fuel (diluted with nitrogen) is injected into hot combustion products of a previous (lean) combustion chamber. The computational results show that the combustion process as well as the NO formation are very sensitive on the mixing intensity. With decreasing mixing intensity the combustion process is stretched out. The ignition delay is shorter but the residence time to achieve complete burnout increases significantly. NO formation rates are lower for less intense mixing and the contributions of the three NO formation channels are shifted from the Fenimore mechanism towards the N_2O and the Zeldovich mechanisms. Nevertheless, total NOx emissions after complete burnout are influenced only slightly, or even tend to decrease with less intense mixing. This is in contrast to the common expectation that imperfect mixing in the combustion process leads to higher NOx emissions.

ACKNOWLEDGEMENT The authors would like to thank Dr R. Corr from the "Regionales Hochschulrechenzentrum" at the University of Kaiserslautern for his kind support and Dr. Michael Streichsbier for fruitful discussions.

References

[1] Chen H., Chen S., Kraichnan R. H. : Probability distribution of stochastically advected scalar field *Physical Review Letters Volume 63, Number 24,* December 1989 pp.2657-2660

[2] Chen J.-Y. : Stochastic Modeling of Partially Stirred Reactors *submitted to Combust. Sci. and Tech.* 3/1995

[3] Chang W.-C., Chen J.-Y. : Impact of Mixing Model on Predicted NO Formation in a Non-premixed Partially Stirred Reactor *Twenty-Sixth Symposium (International) on Combustion* The Combustion Institute, Pittsburgh, to appear 1996

[4] Eswaran V., Pope S.B. : Direct numerical simulations of the turbulent mixing of a passive scalar *Phys. Fluids, Vol.31,No.3,* March 1988

[5] Frenklach M., Wang H., Bowman C.T., Hanson R.K., Smith G.P., Golden D.M., Gardiner W.C., Lissianski V. : An Optimized Kinetic Model for Natural Gas Combustion *25th International Symposium on Combustion, Irvine, California, WIP Poster Session 3, Number 26* (1994)

[6] Bowman C.T., Hanson R.K., Davidson D.F., Gardiner W.C. Jr., Lissianski V., Smith G.P., Golden D.M., Frenklach M., and Goldenberg M. : GRI-Mech 2.1, *http://www.me.berkeley.edu/gri_mech* ,1996

[7] Furuya T., Yamanaka S., Hayata T., Koezuka J., Yoshine T., Ohkoshi A. : Hybrid Catalytic Combustion for Stationary Gas Turbine-Concept and Small Scale Test Results, *ASME Paper 87-GT-99* , 1987.

[8] Hülek T. , Lindstedt R.P.: *Technical Report TF/94/24, MED, Imperial College, London* , 1994

[9] Lutz A.E., Kee R.J., Miller J.A.: *Sandia Report SAND87-8248 UC-4*, 1992

[10] Kee R.J., Rupley F.M., Miller J.A.: *Sandia Report SAND89-8009B UC-706*, 1993

[11] Kraft M., Stöckelmann E., Bockhorn H.: Analysis of wet CO oxidation under turbulent non-premixed conditions using a PDF method and detailed chemical kinetics. *Twenty-Sixth Symposium (International) on Combustion* The Combustion Institute, Pittsburgh, to appear 1996

[12] Miller J.A. , Bowman C.T. : Mechanism and Modeling of Nitrogen Chemistry in Combustion, *Progress in Energy and Combustion Science*, Vol. 15, S. 287-338, 1989.

[13] Nicol D., Malte P.C., Lai J., Marinov N.N., Pratt D.T., Corr R.A.: NOx Sensitivities for Gas Turbine Engines Operated on Lean-Premixed Combustion and Conventional Diffusion Flames, *ASME Paper 92-GT-115*, 1992.

[14] Pope S. B.: PDF Methods for Turbulent Reactive Flows *Progress in Energy and Combustion Science*, Vol.11, pp. 119-192, 1985

[15] Schlegel A.: Experimentelle und Numerische Untersuchungen der NOx-Bildung bei der katalytisch stabilisierten Verbrennung *Diss. ETH Nr. 10887*, (1994)

[16] Valiño L., Dopazo C.: A binomial Langevin model for turbulent mixing *Phys. Fluids* , A3(12), 1991